Biomechanical analysis and new trophic hypothesis for *Riojasuchus tenuisceps*, a bizarre-snouted Late Triassic pseudosuchian from Argentina

JEREMÍAS R.A. TABORDA, M. BELEN VON BACZKO, and JULIA B. DESOJO

Taborda, J.R.A., Belen von Baczko, M., and Desojo, J.B. 2023. Biomechanical analysis and new trophic hypothesis for *Riojasuchus tenuisceps*, a bizarre-snouted Late Triassic pseudosuchian from Argentina. *Acta Palaeontologica Polonica* 68 (X): xxx–xxx.

Ornithosuchids are a Late Triassic pseudosuchian archosaur group, consisting of four species (three from South America, and one from Scotland). All of them have triangular skulls with a protruding premaxilla, large nostrils, an extensive diastema in their narrow snout, a short jaw that does not reach the anterior end of the skull, and serrated posteriorly curved teeth. For this clade, carnivorous and scavenger habits have been previously proposed. Within the Ornithosuchidae, *Riojasuchus tenuisceps* (from Argentina) has the most morphologically extreme characteristics. Based on CT scans of the preserved skulls we generated a 3D model, and over this, we estimated the volumes of the adductors and abductor muscles and the force exerted by each. From these data we built the finite element model and measured the bite force (1.8–2.3 kN). Lateral, tractive, and torsional forces were applied to the end of the snout to evaluate the structural response of the skull during feeding. The results show that *R. tenuisceps* could resist tractive and torsional stresses better than lateral stress. Additionally, we analysed the peculiar morphological characteristics of the skull and their functional implications. We observed that the upper and lower dental rows were laterally separated from each other, preventing the generation of a cutting line during occlusion, and therefore, *R. tenuisceps* would have fed on small-sized prey that it could swallow whole. The curved premaxilla and the short mandible would not allow it to bite with the tip of the snout (ruling out the scavenging hypothesis), but were instead more adequate to capturing prey suspended in a fluid. This set of results allows us to propose that *R. tenuisceps* could have had a zoophagous diet and a wading habit, being able to feed on fish, amphibians, or any small animals that they could catch from the shoreline.

Key words: Archosauria, biomechanics, feeding habits, finite element model, bite force estimation.

Jeremías R.A. Taborda [jeremias.taborda@conicet.gov.ar; ORCID: https://orcid.org/0009-0000-6099-2994], Consejo Nacional de Investigaciones Científicas y Técnicas (CONICET), Godoy Cruz 2290, C1425FQB, Ciudad Autónoma de Buenos Aires, Argentina; Centro de Investigaciones en Ciencias de la Tierra (CICTERRA), Av. Vélez Sarsfield 1611, Ciudad Universitaria, X5016GCA, Córdoba, Argentina.
M. Belen von Baczko [belen_vb@macn.gov.ar; ORCID: https://orcid.org/0000-0003-2570-3418], Consejo Nacional de Investigaciones Científicas y Técnicas (CONICET), Godoy Cruz 2290, C1425FQB, Ciudad Autónoma de Buenos Aires, Argentina; Sección Paleontología de Vertebrados, Museo Argentino de Ciencias Naturales "Bernardino Rivadavia", Av. Ángel Gallardo 470, C1405DJR, Ciudad Autónoma de Buenos Aires, Argentina.
Julia B. Desojo [julideso@fcnym.unlp.edu.ar; ORCID: https://orcid.org/0000-0002-2739-3276], Consejo Nacional de Investigaciones Científicas y Técnicas (CONICET), Godoy Cruz 2290, C1425FQB, Ciudad Autónoma de Buenos Aires, Argentina; División Paleontología Vertebrados, Facultad de Ciencias Naturales y Museo, Universidad Nacional de La Plata, Paseo del Bosque s/n, B1900FWA, La Plata, Argentina.

Received 27 October 2022, accepted 7 July 2023, available online 1 September 2023.

Introduction

During the Triassic (251–201 Ma), a wide diversity of archosaurian forms emerged and radiated, becoming one of the most successful groups of reptiles by the end of this period. Particularly, pseudosuchian archosaurs (the lineage more closely related to crocodiles than birds) exhibited a surprising variety of cranial morphologies, ranging from the flat and long-snouted skulls of phytosaurs and crocodiles, triangular shovel-snouted skulls in most aetosaurs, edentulous jaws possibly covered by a rhamphotheca in some poposauroids, to the high and short crania of rauisuchians

and ornithosuchids (Nesbitt et al. 2013). Particularly within Ornithosuchidae, some bizarre morphologies can be recognized, as their triangular skulls had enlarged overhanging premaxilla with huge nostrils, large diastema in its very narrow snout, and short mandibles that do not reach the anterior end of the skull (Bonaparte 1972; Baczko and Ezcurra 2013; Baczko and Desojo 2016). Currently, this clade is constituted by four species: *Ornithosuchus woodwardi* Newton, 1894, from Scotland, *Riojasuchus tenuisceps* Bonaparte, 1969, and *Venaticosuchus rusconii* Bonaparte, 1970, from Argentina, and *Dynamosuchus collisensis* Müller, Baczko, Desojo, and Nesbitt, 2020, from Brazil, all of which have a different degree of development of their cranial features. Among them, *R. tenuisceps* is the youngest species (from the Los Colorados Formation, Late Triassic of Argentina) and has the most extreme features; it is the ornithosuchid that has been studied in more detail because it is represented by some of the most complete and best preserved specimens known for the group (Bonaparte 1972; Baczko and Desojo 2016; Baczko et al. 2020).

Different feeding habits have been proposed for these ornithosuchids with bizarre skulls based on various sources of information. In 1961, Walker analysed the lines of action of adductor muscles for bite and suggested that the jaw of *O. woodwardi* showed a specialization for the capture of fast-moving prey (Walker 1961). Years later, the same author interpreted *O. woodwardi* as a predatory form because of some anatomical traits (e.g., large curved and serrated teeth, manus with outer digits slightly reduced and better adapted for grasping) and its purportedly large size and bipedal posture (forelimbs shorter and slenderer than hindlimbs, parasagital posture of the hindlimbs, and well-developed anterior trochanter for the iliofemoralis externus muscle) (Walker 1964). However, upon identifying large bite marks on middle-sized rhynchosaur bones from Lossiemouth Formation from the UK, Benton (1983) suggested that these were produced by the ornithosuchid *O. woodwardi*, the largest carnivore known from that locality who might have scavenged on those carcasses. Posteriorly, Bonaparte (1997) presumed a carnivorous diet for *R. tenuisceps* based on its dental morphology and snout specialized for sectioning its prey. More recently, Baczko (2018), followed by Müller et al. (2020), proposed once again a scavenger habit for ornithosuchids, in these cases for *V. rusconii* (from the Ischigualasto Formation, Argentina) and *D. collisensis* (from the Santa Maria Formation, Candelária Sequence, Brazil) based on a geometric biomechanical study and on taphonomical observations respectively.

In order to test these feeding habit hypotheses, it is necessary to analyse the mechanical performance of the ornithosuchid skull. For this, we performed an analysis of continuum mechanics. These studies are based on a mathematical model that allows knowing or predicting the response of a continuous medium (solid or fluid) to external factors depending on its internal properties, that is, for example, the deformation of a solid or the movement of the particles of a fluid. Within this field, one of the most used mathematical models for biomechanical studies is the finite element method (Rayfield 2007; Araujo and Polcyn 2013; Nieto et al. 2021; Taborda et al. 2021). This methodology allows for analyses of a complex structure as a trophic apparatus, and evaluating its mechanical capabilities and performance in different food intake scenarios (Rayfield 2004; Bestwick et al. 2022). For this reason, the finite element method allows us to understand the ecological role of the ornithosuchid *R. tenuisceps* via a quantitative method for the first time.

Institutional abbreviations.—PVL, Paleontología de Vertebrados, Instituto Miguel Lillo, Tucumán, Argentina.

Other abbreviations.—DICOM, Digital Imaging and Communication In Medicine; FEA, Finite Element Analysis; FEm, finite element model; MAB, muscular action bars; MDA, Multi-body Dynamics Analysis.

Material and methods

Two skulls of *Riojasuchus tenuisceps* Bonaparte, 1969, were studied, the holotype PVL 3827 and the referred specimen PVL 3828 (Baczko and Desojo 2016). Both skulls of *R. tenuisceps* preserved the cranium and mandibles in articulation, although they are somewhat deformed (Fig. 1A, B). The skull of the holotype is the most complete, but unfortunately, this specimen has lost the real shape of its teeth by the aggressive mechanical preparation originally performed on it. The skull of PVL 3828 is a little less complete than the holotype, lacking the anterodorsal tip of the snout and having the posterior region of the skull roof crushed. However, PVL 3828 was less damaged during its preparation and preserved the dental morphology intact. The two specimens have a similar size and combining the information provided by both of them we developed a complete 3D virtual model of the skull (Fig. 1C), which was then used to reconstruct the muscles of the adductor chamber and perform the analysis here presented (Baczko et al. 2014; Lautenschlager 2016; Taborda 2016; Baczko 2018; Taborda et al. 2021).

The skulls of *R. tenuisceps* were scanned using Computed Tomography (CT) acquisition methods. The CT data were acquired on a medical axial tomography multi-slicer of

Table 1. Specifications of DICOM (Digital Imaging and Communication In Medicine) series for each scanned specimen of *Riojasuchus tenuisceps*.

Specimen	Number of slices	Slice thickness [mm]	Inter-slice distance [mm]	Field of view [mm]	Power [KV]	Xray tube current [mA]	Exposure time [mseg]	Exposure
PVL 3827	256	1	1	300	120	206	17427	245
PVL 3828	713	0.8	0.4	421	120	279	716	200

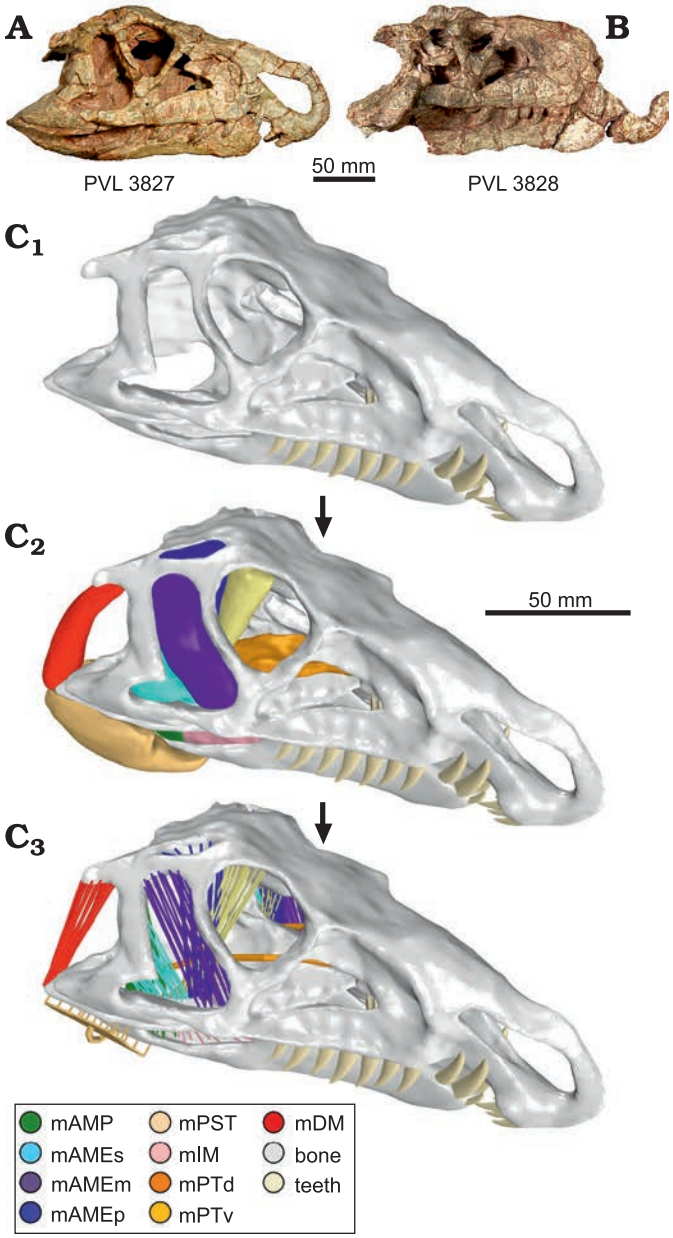

Fig. 1. Skull of the ornithosuchid pseudosuchian *Riojasuchus tenuisceps* Bonaparte, 1969, from Los Colorados Formation, Late Triassic, La Rioja, Argentina. Photographs of the skull of PVL 3827 (**A**) and PVL 3828 (**B**). Reconstructions (**C**). Three-dimensional skull reconstruction (C_1), with muscular reconstruction (C_2), and model of muscular action bars (C_3). Abbreviations: mAMP, musculus adductor mandibulae posterior; mAMEs/m/p, musculus adductor mandibulae externus superficialis/medialis/profundus; mPST, musculus pseudotemporalis; mIM, musculus intramandibularis; mPTv/d, musculus pterygoideus ventralis/dorsalis; mDM, musculus depressor mandibulae. The 3D views of reconstructions are available in the SOM (Supplementary Online Material available at http://app.pan.pl/SOM/app68-Taborda_etal_SOM.pdf).

64-channel; PVL 3827 was scanned at Médicos Asociados de Tucumán, S.A. (Tucumán, Argentina); and PVL 3828 at the Clínica La Sagrada Familia (Buenos Aires, Argentina). DICOM file specifications and associated data obtained for each specimen are detailed in Table 1. For segmentation and 3D model generation, we used the software 3D Slicer v4.1.1 (Fedorov et al. 2012). In order to make a complete virtual skull (Fig. $1C_1$), we aligned and merged all 3D models obtained by segmentation using the CAD softwares Meshmixer v3.4.35, Geomagic Wrap v2017.0.0.111, and Rhinoceros 3D v5. These 3D models were the basis of the biomechanical analysis of the present contribution.

3D skull reconstruction.—Given that the holotype specimen (PVL 3827) has the most complete skull, we used it as base for the virtual skull model. Through the segmentation of the CT scan images, we extracted the sediment that occupied the internal cranial cavities and recovered the cranial elements. Afterwards, we merged the fragments and repaired the plastic deformation of the skull. The dental morphology is better preserved in the skull of PVL 3828 (Baczko and Desojo 2016), and for that reason we reconstructed the 3D teeth based on this specimen. Based on that, we generated the three premaxillary teeth, the seven maxillary teeth, and the nine dentary teeth, which were placed in their corresponding alveolus according to their size. The cranio-mandibular joint was modelled using bars of non-linear material with the property of stretching but not compressing (Table 2). We used these 3D structures to simulate the soft tissue of the joint and allow the independent movements of the cranium and mandible.

Table 2. Setting parameter for the non-linear elastic material.

Strain	Stress
-500	-1000000
-10	-2000
0	0
5	5
1000	1000

Muscular reconstruction and modeling.—The reconstruction of the adductor and abductor musculature in *Riojasuchus tenuisceps* was principally based on the model of the living crocodylians *Caiman yacare*, *Caiman latirostris*, and *Alligator mississippiensis*. (Iordansky 2000; Holliday and Witmer 2007; Bona and Desojo 2011; Holliday et al. 2013; Sellers et al. 2022; Schumacher 1973; Taborda 2016; Taborda et al. 2021). Based on this anatomical information, we reconstructed the musculus adductor mandibulae posterior (mAMP), musculus adductor mandibulae externus superficialis/medialis/profundus (mAMEs/m/p), musculus pseudotemporalis (mPST), musculus intramandibularis (mIM), musculus pterygoideus ventralis/dorsalis (mPTv/d), and musculus depressor mandibulae (mDM). We reconstructed the adductor chamber musculature in 3D using the CAD software Meshmixer v3.4.35 (Fig. $1C_2$). Based on the 3D model we estimated the force of each muscle (Table 3) from their cross-sectional area (Porro et al. 2011) using the methodology described on the supplementary material of Taborda et al. (2021). Usually, the muscular force is applied over the bone surface as a vector (e.g., Ross et al. 2005; Degrange et al. 2010; Porro et al. 2011; Marcé-Nogué et al. 2015; Snively et al. 2015), but we considered that this

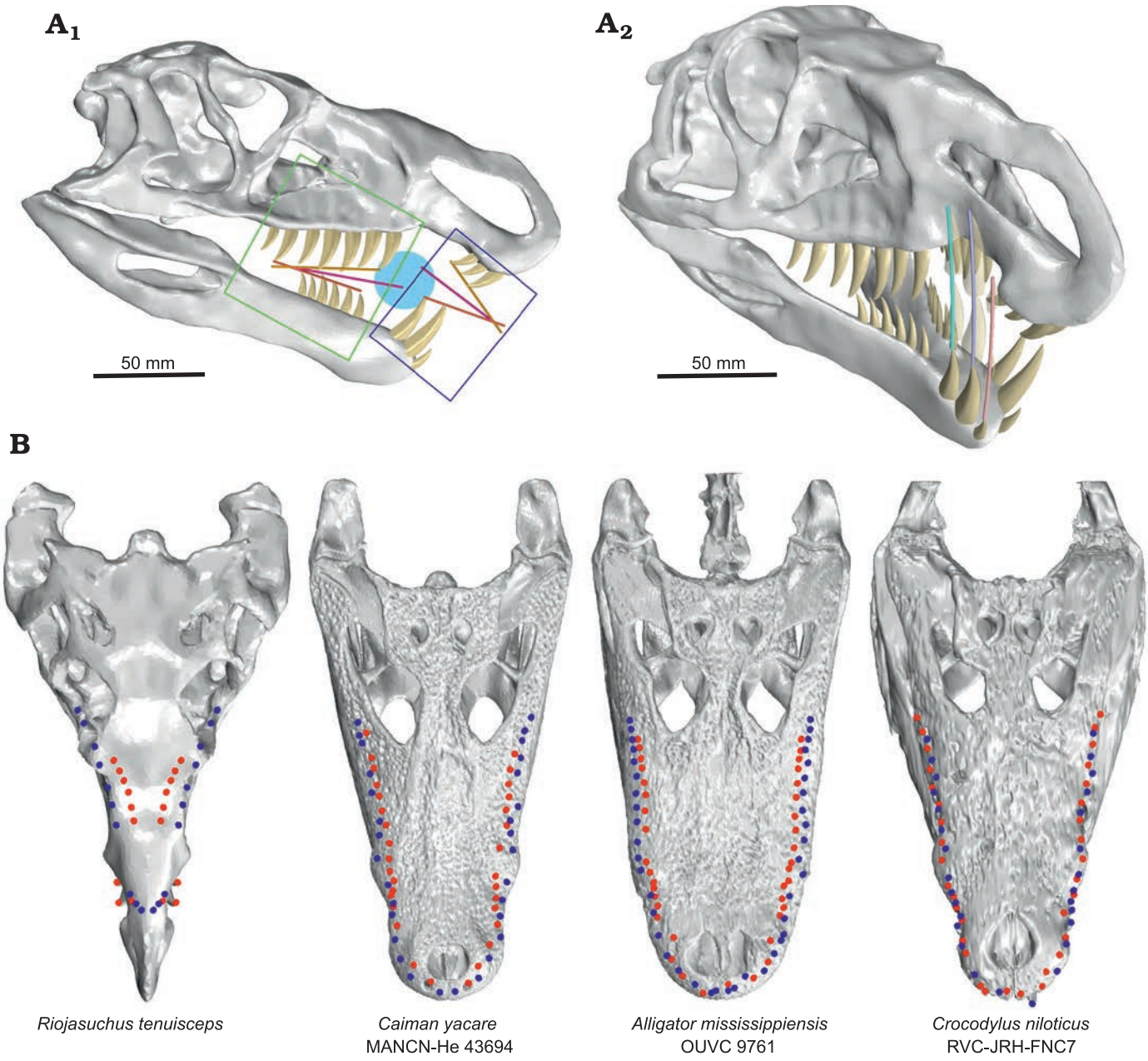

Fig. 2. Analysis of mandibular occlusion in the ornithosuchid pseudosuchian *Riojasuchus tenuisceps* Bonaparte, 1969. **A**. Skull in lateral view (A_1), marking the anterior (blue frame) and posterior (green frame) jaw; also indicated the closing angles for each section of the jaw. The bars show the tendency line of cranial teeth apex (yellow bar), the tendency line of mandibles teeth apex (orange bar), and middle of angle between both (pink bar); the light blue circle represent the captured prey. Arc formed by the anterior dentary teeth during the closing jaw (A_2). **B**. Skulls comparison between *Riojasuchus tenuisceps* and living crocodiles, with teeth apexes plotted in dorsal view. The teeth apexes plot shows the separation between the cranial and mandibular dental rows on the same side. The blue and red dots correspond to the cranium and mandible teeth apexes respectively. B not to scale.

method does not provide a good approximation to the action of real muscles. For this reason, we modelled the muscles using the system of "muscular action bars" (MAB). This consists of a group of bars with the property of contracting (e.g., McHenry et al. 2007; Wroe et al. 2008; Cox et al. 2015; Lautenschlager et al. 2016; Taborda 2016; Taborda et al. 2021), and thus applying force like a real muscle (Fig. $1C_3$). For setting the MABs, we used a theoretical thermo-isotopic material (Taborda 2016; Taborda et al. 2021) whose properties are detailed in Table 3.

Finite element model.—In order to make the finite element model **(**FEm), we considered a priori that the skull of *Riojasuchus tenuisceps* was a completely akinetic structure because no mobile intracranial articulations could be identified (i.e., synovial basal and otic joints, Holliday and Witmer 2008). The skull mesh is composed of tetrahedral elements with four nodes. The elastic properties of the materials that composed the skull model are detailed in Table 4. For the bone elastic properties, we used the closest living ornithosuchid relatives, crocodilians, following the extant

Table 3. Values for the modelling of the adductor chamber muscles. F, estimated muscles; PCSA, estimated physiological cross-sectional area; ε, Young's modulus; ν, Poisson's ratio.

Muscle	PCSA [mm^2]	F musc [N]	ε [GPa]	ν
mAMP	180.01	45	150.01	0.4
mAMEs	309.13	77.28	257.61	0.4
mAMEm	130.54	32.64	108.78	0.4
mAMEp	220.27	55.07	183.56	0.4
mPsT	177.62	44.41	148.02	0.4
mIM	163.39	40.85	136.16	0.4
mPTd	283.17	70.79	235.98	0.4
mPTv	831.40	207.85	692.84	0.4
mDM	110.27	27.57	91.89	0.4

Table 4. Material properties. ε, Young's modulus; ν, Poisson's ratio.

Tissue	Material type	ε [GPa]	ν
Bone	Elastic	13 300	0.4
Tooth	Elastic	60 400	0.31
Transiliens cartilage	Elastic	0.010	0.3

phylogenetic bracketing method (Witmer 1995), therefore, we assigned the average value obtained from the mandible of *Alligator mississippiensis* (Zapata et al. 2010). For teeth, we used the Young's Modulus based on the value measured in fresh crocodilian teeth (Creech 2004). For the interpretation of our results, we assumed the bone shear modulus as 3.6 GPa and considered a maximum stress normal condition (safety factor) around 1.8 GPa (Taborda et al. 2021).

The FEm was fixed (restricting all degrees of freedom) at the articular surface of occipital condyle and the attachment surfaces of neck muscles (musculus transversospinalis capitis and musculus splenius capitis). The rest of the boundary conditions are explained below for each analysis. We used the software FEMAP v10.3.1 to perform the FEm and the software ADINA v8.7.3 to solve the system.

Dental and occlusion analysis.—To analyse the teeth configuration, we divided the jaw in two sections: anterior (consisting of premaxillary teeth and the first three teeth of dentary) and posterior (that consists of maxillary teeth and dentary teeth 4–9). This split is based on the natural division of teeth row by the premaxillary and dentary diastema (Fig. $2A_1$).

The teeth of *Riojasuchus tenuisceps* are laterally compressed with distally curved apex, and carinae with denticles on both mesial and distal margins (Baczko and Desojo 2016). Although the teeth have the typical blade-like morphology, *R. tenuisceps* would not have been able to cut its prey with a bite because the cranial and mandibular dental rows on the same side are well separated from each other (Fig. 2B). In the posterior section of the jaw, we can observe that the apex of teeth in the maxillary and dentary row on the same side are separated by 9.4 mm; its distance is similar to that between the tooth rows of the two hemimandibles: 12.2 mm. For this reason, the jaw of *R. tenuisceps* lacks a cutting line as happens in some living crocodiles. In the latter (e.g., *Alligator mississippiensis*) the upper and lower teeth are quite aligned, and in some cases, they even interdigitate (e.g., *Crocodylus niloticus*) (Fig. 2B). This causes a die cut line (or dotted line) to be generated on the bite, making it easier to section large prey. However, there are other cases, such as in *C. yacare,* where the upper teeth are less aligned with the lower ones and therefore (Fig. 2B), they resort to feeding on small prey that they can swallow whole without having to cut it (Santos et al. 1996).

In the anterior tooth section of *R. tenuisceps*, the dentary teeth are positioned on the labial side of the premaxillary diastema, just behind the premaxillary teeth. On the other hand, the premaxillary teeth are oriented distally (according to Smith and Dodson 2003), pointing towards the interior of the mouth. If we observe the arc formed by the anterior dentary teeth during the occlusion, we can see that they do not pass close enough to the premaxillary teeth to generate a cutting line (Fig. $2A_2$).

The shorter mandible and the orientation of premaxillary teeth would make it impossible for *R. tenuisceps* to grab and/or pluck pieces of prey or carrion with the snout tip. Moreover, the impossibility of cutting with posterior tooth rows suggests that *R. tenuisceps* would have had to swallow its prey whole, reducing the possible size ranges of this.

Additionally, we analysed the angles formed between the upper and lower dental rows in the anterior and posterior jaw during its closure. For these, we generated (by least squares) a trend line for the tooth apexes, in upper and lower dental rows from anterior and posterior jaw independently, and we observed the angles formed in each section of the jaw (Fig. $2A_1$). In the posterior jaw, the jaw occlusion occurs from back to front; whereas in the anterior jaw the morphology and arrangement of the teeth causes the mouth to close from front to back. And although the jaw configuration would not allow *R. tenuisceps* to cut or tear its prey, it would be more suitable for catching small animals suspended in a fluid because this closing mechanism favours the "ensnaring" of prey in the middle of the jaw (Fig. $2A_1$).

Biomechanical analysis

Bite force simulation.—For the FEA, the bite force is commonly estimated from other measurements (e.g., skull size or body mass, among others), and incorporated to model as boundary condition (e.g. Ross et al. 2005; Degrange et al. 2010; Porro et al. 2011; Marcé-Nogué et al. 2015; Snively et al. 2015). However, in our study we measure the bite force directly as a result of the analysis similar to how it is measured in a living individual. To obtain the bite force, we fixed some points in certain positions along the jaw (Fig. 3) during the bite simulation (that is, when the MABs contract) and measured the reaction force at each point. The total bite force, in each place of the jaw, is obtained by adding the modulus of all reaction forces at the fixed points for simultaneous measurement (Taborda et al. 2021). A similar

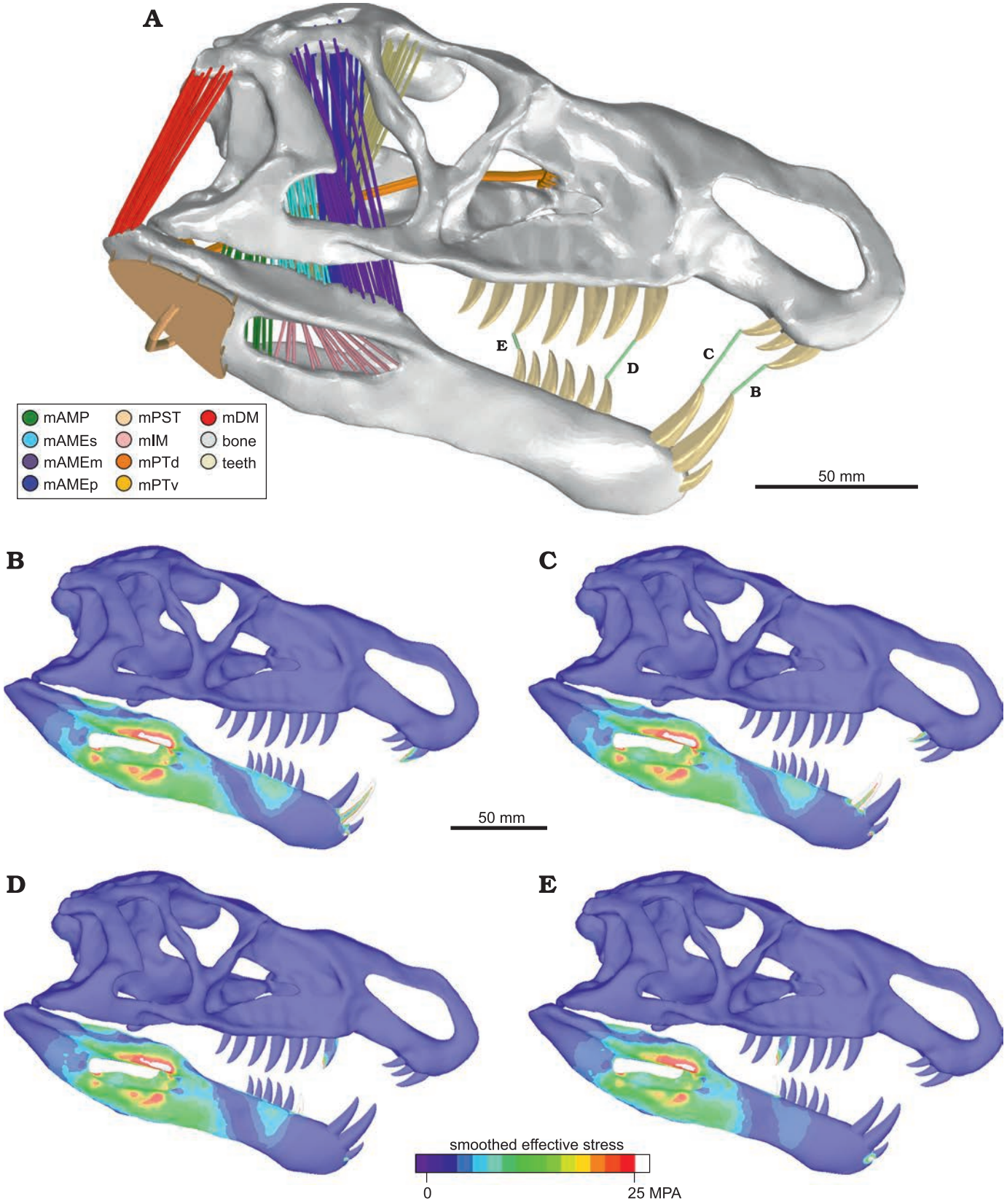

Fig. 3. Biomechanical test of bite force in the ornithosuchid pseudosuchian *Riojasuchus tenuisceps* Bonaparte, 1969. Skull model in lateral view (**A**) indicating the position of the bite force measurements (**B**–**E**), showing the respective results of finite element analysis for each bite force test. Abbreviations: mAMP, musculus adductor mandibulae posterior; mAMEs/m/p, musculus adductor mandibulae externus superficialis/medialis/profundus; mPST, musculus pseudotemporalis; mIM, musculus intramandibularis; mPTv/d, musculus pterygoideus ventralis/dorsalis; mDM, musculus depressor mandibulae. The colorimetric scale shows the smooth effective stress distribution in the structure.

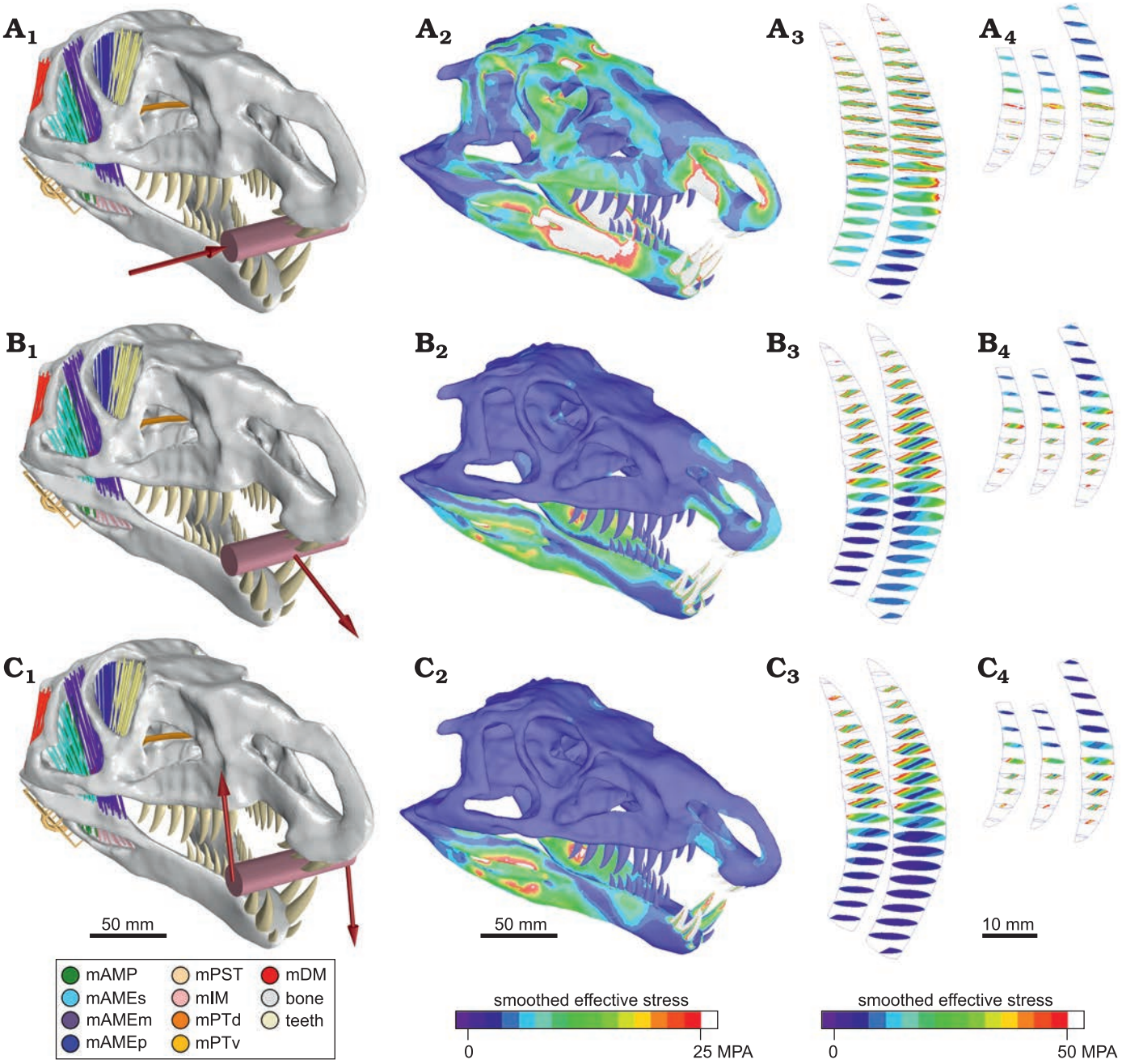

Fig. 4. Biomechanical test of external force in the ornithosuchid pseudosuchian *Riojasuchus tenuisceps* Bonaparte, 1969. Lateral load force (**A**), tractive load force (**B**), and twist force (**C**). External force configuration for each test. The red arrows indicate the direction of the applied forces and the pink cylinder represents the bitten mass (A_1–C_1). For each test, we present the result of finite element analysis on anterolateral view of the skull (A_2–C_2), sections of the second and third right teeth of the dentary (A_3–C_3), and sections of right premaxillary teeth (A_4–C_4). Abbreviations: mAMP, musculus adductor mandibulae posterior; mAMEs/m/p, musculus adductor mandibulae externus superficialis/medialis/profundus; mPST, musculus pseudotemporalis; mIM, musculus intramandibularis; mPTv/d, musculus pterygoideus ventralis/dorsalis; mDM, musculus depressor mandibulae. The colorimetric scale shows the smooth effective stress distribution in the structure.

FEA method for measurement the bite force was tested and compared results with in vivo bite force measurement in crocodiles (Sellers et al. 2017). In this analysis, the authors observed a good alignment of the bite force estimation with that observed in vivo for middle sized individuals, but for large and small size specimens the error increases. However, the methodology for modelling and setting the boundary conditions described by Taborda et al. (2021) allowed us to obtain a better result for bite force. Other research about estimation of bite force using Multi-body Dynamics Analysis (MDA) (Curtis et al. 2010, 2013; Bates and Falkingham 2012; Gröning et al. 2013) obtained similar values to those measured in living diapsids. These results support the validity of this technique to measure bite forces.

In the case of *Riojasuchus tenuisceps*, we only considered the bilateral bite force because the snout is remarkably

Table 5. Bite force measured with FEA in different points of jaw. The position of these points are indicated in Fig. 3. Abbreviations: D#, dentary teeth; Mx#, maxillary teeth; PrMx#, premaxillary teeth.

Point	Teeth	Bite force [N]
B	PrMx1 – D2	1866.9
C	PrMx3 – D3	1981
D	Mx1 – D4	2058.5
E	Mx5 – D9	2371.7

narrow and the tooth rows are closely spaced, and in the posterior jaw the tooth rows of the mandible and cranium of the same side are laterally separated from each other. The bite force measurement was performed at four positions in the jaw (Fig. 3A) and the results obtained for each position in the jaw of *R. tenuisceps* are detailed in Table 5. The obtained bite force is similar to that measured by Erickson et al. (2012) for *Caiman latirostris* (1.67 kN for caniniform and 2.42 kN for molariform).

The results of the model do not show areas with high stress values in the cranium or mandible. The obtained maximum stress values (≈150 MPa) were very low compared with the safety factor (1.8 GPa). This confirms that there are no areas of important kinesis acting in the skull during biting. During all bite force tests, no stress concentrations were observed in the skull, whereas in the mandible, the maximum stress was concentrated in the area around the mandibular fenestra (Fig. 3B–E). These results highlight the importance of the surangular shelf to maintain the structural integrity of the mandible.

Skull reaction to external force in the jaw during the bite.—In order to analyse the stress pattern during capture of food, we recorded the response of the skull in different situations of external force (lateral load force, tractive load force, and twist force) applied in the anterior jaw (Fig. 4).

For all tests we applied 1 kN load force; this value is approximately half the average bite force measured here. This force value was equally distributed among all the load points of each test. The results obtained in all tests show very low maximum stress values compared to the safety factor, thus, we considered that the animal would not be injured in these situations.

Lateral load force.—This setting corresponds to movements caused by live prey attempting to escape. In this situation, the prey would exert a lateral force perpendicular to the sagittal plane of the skull (Fig. 4A). This scenario was used to evaluate the ability of *Riojasuchus tenuisceps* to capture live prey.

In the mandible, the stress is mainly concentrated anterior to the mandibular fenestra, on the lingual surface. In the cranium, the stress is accumulated on the area of the diastema, on the palatal face of the premaxillae (Fig. $4A_1$). In the teeth, the stress is concentrated in the central area of the lingual and labial surfaces along all crow (Fig. $4A_2$, A_3). Because the teeth are laterally compressed, these are weaker in the transverse direction. Therefore, this type of effort would not be desirable in these structures.

Tractive load force.—The purpose of this scenario was to evaluate the performance of *Riojasuchus tenuisceps* during the pullback of a prey with its jaws. In this case, the forces over the skull are mainly longitudinal, and therefore, the load forces are applied in longitudinal direction (Fig. 4B).

The result shows that the stress distribution is concentrated around the mandibular fenestra and the premaxillary diastema (Fig. $4B_1$). This pattern may look similar to that obtained in the previous test, but the intensity is remarkably smaller than that one. Contrary to the result of the lateral load force test, the stress in the teeth is distributed over the mesial and distal carinae (Fig. $4B_2$, B_3). The teeth of *R. tenuisceps* would better resist the stress in this direction than in the transverse direction.

Twist force reaction.—If *Riojasuchus tenuisceps* were to pull a prey out of the water, a torque would be experienced applied to the jaw. To evaluate the structural response of the skull during this situation, we performed a test applying external bilaterally opposed forces (i.e., ascending on the right side and descending on the left side) on the anterior jaw during the bite (Fig. 4C).

The obtained stress distribution pattern in cranium and mandible (Fig. $4C_1$) is similar to that of the previous test (tractive load force). However, the most noticeable difference is located on the stress pattern displayed by the teeth. Although stress is also located in both carinae, the mesial margin shows higher stress values than the distal one (Fig. $4C_2$, C_3). This distribution is consistent with the dental morphology since a vertical force at the apex compresses the mesial margin (concave) and distends the distal margin (convex). It was also observed that the teeth with the ascending load show a major increase in stress compared to descending loaded teeth. But this effect is expected because of the asymmetry of the loading force; while on the left side (descending load) the elastic articulation cranio-mandibular helps to dissipate stress, in the ascending load side (right) the stress is absorbed by the teeth. The maximum stress values are much lower than the assumed safety factor (1.8 GPa), so they would not represent a danger to the animal while feeding.

Comparing the results of the external load force test, we interpret that the skull of *R. tenuisceps* could better resist traction and torque efforts than that produced by lateral load force.

Concluding remarks

A previous quantitative functional analysis concluded that ornithosuchids probably had a strong bite, but with low speed (Baczko 2018). In that analysis, the author considers that these results would not support hunting abilities, but would be more appropriate for animals with scavenger hab-

its. However, said study only bases its conclusions on the results of one-dimensional lever arms and did not consider other relevant anatomical information (e.g., the recurved premaxilla, and separation between tooth rows). In the case of *Riojasuchus tenuisceps*, the recurved premaxilla would impede biting with the tip of the snout, and the separation between tooth rows would only permit swallowing its prey whole. For this reason, we discard the scavenger habit previously proposed for *R. tenuisceps*.

The teeth of *R. tenuisceps* have the typical "ziphodont tooth'' morphology seen in other carnivorous archosaurs (often interpreted as active hunting animals) like those of basal loricatans and theropod dinosaurs (Tsuihiji et al. 2013). However, the particular tooth configuration in the jaws of *R. tenuisceps* does not agree with that of hunting or scavenger habits because the short jaw with hypertrophied teeth that fit into a diastema would not allow it to cut through or tear apart its prey. Nevertheless, with its teeth working like a trap, the jaws of *R. tenuisceps* appear to be ideal for catching small animals if suspended in a fluid, where its anteroventrally projected premaxillae would not be a hindrance for capturing prey.

In turn, analysing the spearhead shape of the skull of *R. tenuisceps*, we can observe that it is more hydrodynamically apt for frontal movements than for lateral movements. This is probably because the skull is high in lateral view and would cause great resistance when moving laterally. Whereas performing a frontal movement, the wedge shape of the skull (in dorsal view) would allow it to easily displace fluids to the sides, like the prow of a ship, decreasing resistance. This is consistent with our result of the biomechanical analysis that showed both the skull and teeth would be better prepared for resisting tractive and twisting forces, while they are less resistant to lateral forces.

The particular tooth configuration, the jaw morphology, its biomechanical capabilities, and the fact that it could probably have only swallowed prey whole, leads us to think that *R. tenuisceps* could have had a wading habit, being able to feed mainly on fish, amphibians, or any small animal that they could capture in the water. Taking into account the biomechanical and hydrodynamic capabilities of the skull, we think that *R. tenuisceps* would not be likely to capture its prey during diving and performing aggressive lateral movements like its closest living relatives, the crocodiles. Instead, we propose that *R. tenuisceps* would do so in the manner of wading birds, standing on the edge of a water body and making quick attacks from above by submerging its head.

A similar feeding behaviour has been proposed for the theropod dinosaur *Spinosaurus aegyptiacus* (Cuff and Rayfield 2013; Henderson 2018; Hone and Holtz 2021), which also has a slightly curved premaxilla, a narrow snout, and short mandible. Interestingly, *S. aegyptiacus* also has a longer snout and set back nostrils like modern wading birds (Hone and Holtz 2021), giving it an advantage for foraging in the water for a long time while keeping the nostrils outside for breathing. In the case of *R. tenuisceps*, the nares are in laterally position near the tip of the snout, and therefore would not allow it the same foraging behaviour. However, this position of the nostrils is not a limitation for a fishing habit, but would only restrict it to fast movements with short periods of head immersion.

Additionally, the non-archosaurian archosauriform *Proterosuchus fergusi* appears to share some of the anatomical traits seen in *R. tenuisceps*, such as the downturned snout that is determinant for prey catching on both species even though they do not have the same life habit. *Proterosuchus fergusi* is thought to be semi-aquatic, and therefore feed mostly in water bodies based on the presence of horizontal zygapophyses, high and laterally compressed tail, limb proportions, and the shape of the labyrinth (Broom 1903; Broili and Schröder 1934; Reig 1970; Cruickshank et al. 1972; Brown et al. 2019). When analysing the caudal vertebrae of PVL 3828 of *R. tenuisceps*, we can observe that the tall neural spines grant it a laterally compressed tail (Baczko et al. 2020: fig. 5E), which might be interpreted as the only adaptation of *R. tenuisceps* for moving in water like *P. fergusi*. Although the zygapophyses are oriented at 45º and not in a horizontal position as in *P. fergusi*, the condition of *R. tenuiceps* resembles that of living crocodiles, which also have semi aquatic habits and propel through water with powerful tail movements.

In sum, it is possible that the combination of features seen in *R. tenuisceps* would allow it, when needed, to propel in a body of water as modern crocodiles do nowadays. However, the erect stance of *R. tenuisceps* differs from the sprawling posture of *P. fergusi*, making the former better adapted for terrestrial habits (Parrish 1986). Moreover, some authors have proposed that the ornithosuchids could be facultative bipedal animals (e.g., Walker 1964; Bonaparte 1997), which would be convenient for a wading habit. This would allow it to move more comfortably along the banks and shallow flooded areas of the Los Colorados Formation (Santi Malnis et al. 2020) and have better vision while in search of food. These locomotory hypotheses are currently being tested, whose results could support the new feeding habit here proposed for *R. tenuisceps*.

Acknowledgments

We thank the curators Jaime Powell and Pablo Ortiz (both the Instituto Miguel Lillo, Tucuman, Argentina) for allowing access to the specimens under their care. We thank the technicians of Clínica La Sagrada Familia and Médicos Asociados de Tucumán, S.A. for their assistance while carrying out the CT-scans of the specimens. We also thank Andre Rowe (University of Bristol, UK), the anonymous reviewer and the editor Daniel E. Barta (Oklahoma State University Center for Health Sciences, Tahlequah, USA) for their comments and suggestions on this manuscript. This research was funded by Agencia Nacional de Promoción Científica y Tecnológica (AGENCIA I+D+i) through PICT 2018-0717 (JBD) and 2018-0853 (BvB).

References

Araújo, R. and Polcyn, M.J. 2013. A biomechanical analysis of the skull and adductor chamber muscles in the Late Cretaceous plesiosaur Libonectes. *Palaeontologia Electronica* 16 (2): 10A.

Baczko, M.B. von 2018. Rediscovered cranial material of *Venaticosuchus rusconii* enables the first jaw biomechanics in Ornithosuchidae (Archosauria: Pseudosuchia). *Ameghiniana* 55: 365–379.

Baczko, M.B. von, and Ezcurra, M.D. 2013. Ornithosuchidae: a group of Triassic archosaurs with a unique ankle joint. *Geological Society, London, Special Publications* 379 (1): 187–202.

Baczko, M.B. von, Taborda, J.R.A., and Desojo, J.B. 2014. First biomechanical analysis on the skull of the ornithosuchid *Riojasuchus tenuisceps* Bonaparte from the Los Colorados Formation, Late Triassic of Argentina. *Ameghiniana* 51 (6R): 23.

Baczko, M.B. von and Desojo, J.B. 2016. Cranial anatomy and palaeoneurology of the archosaur *Riojasuchus tenuisceps* from the Los Colorados Formation, La Rioja, Argentina. *Plos One* 11 (2): e0148575.

Baczko, M.B. von, Desojo, J.B., and Ponce, D. 2020. Postcranial anatomy and osteoderm histology of *Riojasuchus tenuisceps* and a phylogenetic update on Ornithosuchidae (Archosauria, Pseudosuchia). *Journal of Vertebrate Paleontology* 39 (5): 1–25.

Bates, K.T. and Falkingham, P.L. 2012. Estimating maximum bite performance in *Tyrannosaurus rex* using multi-body dynamics. *Biology Letters* 8: 660–664.

Benton, M.J. 1983. The Triassic reptile Hyperodapedon from Elgin: functional morphology and relationships. *Philosophical Transactions of the Royal Society B: Biological Sciences* 302: 379–430.

Bestwick, J., Jones, A.S., Nesbitt, S.J., Lautenschlager, S., Rayfield, E.J., Cuff, A.R., Button, D.J., Barrett, P.M., Porro, L.B., and Butler, R.J. 2022. Cranial functional morphology of the pseudosuchian Effigia and implications for its ecological role in the Triassic. *Anatomical Record* 305 (10): 2435–2462.

Bona, P. and Desojo, J.B. 2011. Osteology and cranial musculature of *Caiman latirostris* (Crocodylia: Alligatoridae). *Journal of Morphology* 272: 780–795.

Bonaparte, J.F. 1969. Dos nuevas "faunas" de reptiles triásicos de Argentina. *In*: A.J. Amos (ed.), *La Estratigrafia del Gondwana: coloquio de la UICG (1st International Symposium on Gondwana Stratigraphy and Paleontology, Buenos Aires, 1967)*, 283–325. Paris.

Bonaparte, J.F. 1970. Annotated list of the South American Triassic tetrapods. *Gondwana Symposium Proceedings and Papers* 2: 665– 682.

Bonaparte, J.F. 1972. Los Tetrápodos del sector Superior de la Formación Los Colorados (Triásico Superior). I Parte. *Opera Lilloana* 22: 1–183.

Bonaparte, J.F. 1997. *El Triásico de San Juan – La Rioja Argentina y sus Dinosaurios. 1st Edition*. 190 pp. Museo Argentino de Ciencias Naturales "Bernardino Rivadavia", Buenos Aires.

Broili, F. and Schröder, J. 1934. Beobachtungen an Wirbeltieren der Karroo Formation. V. Uber *Chasmatosaurus vanhoepeni* Haughton. *Sitzungsberichte der Bayerischen Akademie der Wissenschaften, Mathematisch-Naturwissenschaftliche Abteiliung* 3: 225–264.

Broom, R. 1903. On a new reptile (*Proterosuchus fergusi*) from the Karroo beds of Tarkastad, South Africa. *Annals of the South African Museum* 4: 159–164.

Brown, E.E., Butler, R.J., Ezcurra, M.D., Bhullar, B.A.S., and Lautenschlager, S. 2019. Endocranial anatomy and life habits of the Early Triassic archosauriform *Proterosuchus fergusi*. *Palaeontology* 63: 255–282.

Cox, P.G., Rinderknecht, A. and Blanco, R.E. 2015. Predicting bite force and cranial biomechanics in the largest fossil rodent using finite element analysis. *Journal of Anatomy* 226: 215–223.

Creech, J.E. 2004. *Phylogenetic Character Analysis of Crocodylian Enamel Microstructure and its Relevance to Biomechanical Performance*. 70 pp. Unpublished MSc. Thesis, Florida State University, Tallahassee.

Cruickshank, A.R.I., Joysey, K.A., and Kemp, T.S. 1972. The proterosuchian thecodonts. *Studies in Vertebrate Evolution* 89 (1): 19.

Cuff, A. R. and Rayfield, E. J. 2013. Feeding mechanics in spinosaurid theropods and extant crocodilians. *PLoS ONE* 8 (5): e65295.

Curtis, N., Jones, M.E.H., Evans, S.E., O'Higgins, P., and Fagan, M.J. 2013. Cranial sutures work collectively to distribute strain throughout the reptile skull. *Journal of the Royal Society, Interface/the Royal Society* 10 (86): 20130442.

Curtis, N., Jones, M.E.H., Evans, S.E., Shi, J., O'Higgins, P., and Fagan, M.J. 2010. Predicting muscle activation patterns from motion and anatomy: modelling the skull of *Sphenodon* (Diapsida: Rhynchocephalia). *Journal of the Royal Society, Interface/the Royal Society* 7: 153–160.

Degrange, F.J., Tambussi, C.P., Moreno, K., Witmer, L.M., and Wroe, S. 2010. Mechanical analysis of feeding behavior in the extinct 'terror bird' *Andalgalornis steulleti* (Gruiformes: Phorusrhacidae). *PloS One* 5 (8): e11856.

Erickson, G.M., Gignac, P.M., Steppan, S.J., Lappin, A.K., Vliet, K.A., Brueggen, J.D., Inouye, B.D., Kledzik, D., and Webb, G.J.W. 2012. Insights into the ecology and evolutionary success of crocodilians revealed through bite-force and tooth-pressure experimentation. *PLoS ONE* 7 (3): e31781.

Fedorov, A., Beichel, R., Kalpathy-Cramer, J., Finet, J., Fillion-Robin, J.C., Pujol, S., Bauer, C., Jennings, D., Fennessy, F., Sonka, M., Buatti, J., Aylward, S., Miller, J. V., Pieper, S. and Kikinis, R. 2012. 3D Slicer as an image computing platform for the Quantitative Imaging Network. *Magnetic Resonance Imaging* 30: 1323–1341.

Gröning, F., Jones, M.E.H., Curtis, N., Herrel, A., O'Higgins, P., Evans, S.E., and Fagan, M.J. 2013. The importance of accurate muscle modelling for biomechanical analyses: a case study with a lizard skull. *Journal of the Royal Society, Interface/the Royal Society* 10 (84): 20130216.

Henderson, D.M. 2018. A buoyancy, balance and stability challenge to the hypothesis of a semi-aquatic *Spinosaurus* Stromer, 1915 (Dinosauria: Theropoda). *PeerJ* 6: e5409.

Holliday, C.M. and Witmer, L.M. 2007. Archosaur adductor chamber evolution: Integration of musculoskeletal and topological criteria in jaw muscle homology. *Journal of Morphology* 268: 457–484.

Holliday, C.M. and Witmer, L.M. 2008. Cranial kinesis in dinosaurs: intracranial joints, protractor muscles, and their significance for cranial evolution and function in diapsids. *Journal of Vertebrate Paleontology* 28: 1073–1088.

Holliday, C.M., Tsai, H.P., Skiljan, R.J., George, I.D., and Pathan, S. 2013. A 3D interactive model and atlas of the jaw musculature of *Alligator mississippiensis*. *PLoS ONE* 8(6): e62806.

Hone, D.W. and Holtz Jr, T.R. 2021. Evaluating the ecology of *Spinosaurus*: Shoreline generalist or aquatic pursuit specialist? *Palaeontologia Electronica* 24 (1): a03.

Iordansky, N. 2000. Jaw muscles of the crocodiles: structure, synonymy, and some implications on homology and functions. *Russian Journal of Herpetology* 7: 41–50.

Lautenschlager, S. 2016. Reconstructing the past: methods and techniques for the digital restoration of fossils. *Royal Society Open Science* 3 (10): 160342.

Lautenschlager, S., Brassey, C.A., Button, D.J., and Barrett, P.M. 2016. Decoupled form and function in disparate herbivorous dinosaur clades. *Scientific Reports* 6: 26495.

Marcé-Nogué, J., Fortuny, J., De Esteban-Trivigno, S., Sánchez, M., Gil, L., and Galobart, À. 2015. 3D Computational Mechanics Elucidate the Evolutionary Implications of Orbit Position and Size Diversity of Early Amphibians. *Plos One* 10 (6): e0131320.

McHenry, C.R., Wroe, S., Clausen, P.D., Moreno, K., and Cunningham, E. 2007. Supermodeled sabercat, predatory behavior in *Smilodon fatalis* revealed by high-resolution 3D computer simulation. *Proceedings of the National Academy of Sciences of the United States of America* 104 (41): 16010–16015.

Müller, R.T., Baczko, M.B. Von, Desojo, J.B., and Nesbitt, S.J. 2020. The first ornithosuchid from Brazil and its macroevolutionary and phylogenetic implications for Late Triassic faunas in Gondwana. *Acta Palaeontologica Polonica* 65: 1–10.

Nesbitt, S.J., Brusatte, S.L., Desojo, J.B., Liparini, A., de Franca, M.A.G., Weinbaum, J.C., and Gower, D.J. 2013. Rauisuchia. *Geological Society, London, Special Publications* 379 (1): 241–274.

Nieto, M.N., Degrange, F.J., Sellers, K.C., Pol, D., and Holliday, C.M. 2021. Biomechanical performance of the cranio-mandibular complex of the small notosuchian *Araripesuchus gomesii* (Notosuchia, Uruguaysuchidae). *The Anatomical Record* 305 (10): 2695–2707.

Parrish, J.M. 1986. Locomotor adaptations in the hind limb and pelvis of the Thecodontia. *Hunteria* 1: 3–35.

Porro, L.B., Holliday, C.M., Anapol, F., Ontiveros, L.C., Ontiveros, L.T., and Ross, C.F. 2011. Free body analysis, beam mechanics, and finite element modeling of the mandible of *Alligator mississippiensis*. *Journal of Morphology* 272: 910–937.

Rayfield, E.J. 2004. Cranial mechanics and feeding in *Tyrannosaurus rex*. *Proceedings of the Royal Society B: Biological Sciences* 271: 1451–1459.

Rayfield, E.J. 2007. Finite element analysis and understanding the biomechanics and evolution of living and fossil organisms. *Annual Review of Earth and Planetary Sciences* 35: 541–576.

Reig, O.A. 1970. The Proterosuchia and the early evolution of the archosaurs; an essay about the origin of a major taxon. *Bulletin of the Museum of Comparative Zoology* 139: 229–292.

Ross, C.F., Patel, B. a, Slice, D.E., Strait, D.S., Dechow, P.C., Richmond, B.G., and Spencer, M.A. 2005. Modeling masticatory muscle force in finite element analysis: sensitivity analysis using principal coordinates analysis. *The Anatomical Record. Part A, Discoveries in Molecular, Cellular, and Evolutionary Biology* 283: 288–299.

Santi Malnis, P., Colombi, C.E., Rothis, L.M., and Alcober, O. 2020. Fluvial architecture and paleoenvironmental evolution of the Los Colorados Formation (Norian): Postrift stage of the Ischigualasto-Villa Unión Basin, NW Argentina. *Journal of Sedimentary Research* 90: 1436–1462.

Santos, S.A., Stoll, M., Silva, M., Campos, Z., Magnusson, W.E., and Mourão, G. 1996. Diets of *Caiman crocodilus yacare* from different habitats in the Brazilian Pantanal. *Herpetological Journal* 6: 111–117.

Sellers, K.C., Middleton, K.M., Davis, J.L., and Holliday, C.M. 2017. Ontogeny of bite force in a validated biomechanical model of the American alligator. *The Journal of Experimental Biology* 220: 2036–2046.

Sellers, K.C., Nieto, M.N., Degrange, F.J., Pol, D., Clark, J.M., Middleton, K.M., and Holliday, C.M. 2022. The effects of skull flattening on suchian jaw muscle evolution. *The Anatomical Record* 305 (10): 2791–2822.

Schumacher, G.-H. 1973. The head muscles and hyolaryngeal skeleton of turtles and crocodilians. *In*: C. Gans and T.S. Parsons (eds.), *Biology of the Reptilia. Volume 4. Morphology D*, 101–200. Academic Press, New York.

Smith, J.B. and Dodson, P. 2003. A proposal for a standard terminology of anatomical notation and orientation in fossil vertebrate dentitions. *Journal of Vertebrate Paleontology* 23: 1–12.

Snively, E., Fahlke, J.M. and Welsh, R.C. 2015. Bone-breaking bite force of *Basilosaurus isis* (Mammalia, Cetacea) from the Late Eocene of Egypt estimated by finite element analysis. *PLoS ONE* 10 (2): 1–23.

Taborda, J.R.A. 2016. *Estructura y función cráneodentaria: un acercamiento a la paleobiología de los aetosaurios sudamericanos (archosauria: pseudosuchia).* 203 pp. Unpublished Ph.D. Thesis, Universidad de Buenos Aires, Buenos Aires.

Taborda, J.R.A., Desojo, J., and Dvorkin, E. 2021. Biomechanical skull study of the aetosaur *Neoaetosauroides engaeus* using finite element analysis. *Ameghiniana* 58: 401–415.

Tsuihiji, T., Komatsu, T., Manabe, M., Miyake, Y., Aramaki, M., and Sekiguchi, H. 2013. Theropod tooth from the Upper Cretaceous Himenoura Group in the Koshikijima Islands, southwestern Japan. *Paleontological Research* 17: 39–46.

Walker, A.D. 1961. Triassic reptiles from the Elgin area: *Stagonolepis*, *Dasygnathus* and their allies. *Philosophical Transactions of the Royal Society of London. Series B, Biological Sciences* 244: 103–204.

Walker, A.D. 1964. Triassic reptiles from the Elgin area: *Ornithosuchus* and the origin of carnosaurs. *Philosophical Transactions of the Royal Society B: Biological Sciences* 248: 53–134.

Witmer, L.M. 1995. The extant phylogenetic bracket and the importance of reconstructing soft tissue in fossils. *In*: J.J. Thomason (ed.), *Functional Morphology in Vertebrate Paleontology*, 19–33. Cambridge University Press, Cambridge.

Wroe, S., Huber, D.R., Lowry, M., McHenry, C., Moreno, K., Clausen, P., Ferrara, T.L., Cunningham, E., Dean, M.N., and Summers, A.P. 2008. Three-dimensional computer analysis of white shark jaw mechanics: How hard can a great white bite? *Journal of Zoology* 276: 336–342.

Zapata, U., Metzger, K., Wang, Q., Elsey, R.M., Ross, C.F., and Dechow, P.C. 2010. Material properties of mandibular cortical bone in the American alligator, *Alligator mississippiensis*. *Bone* 46: 860–867.